Continental Shelf Research 212 (2021) 104293

Contents lists available at ScienceDirect

Continental Shelf Research

journal homepage: http://www.elsevier.com/locate/csr

Groundwater chemistry and Sr isotope ratios shed light on connectivity and water-rock interactions in the coastal aquifer of the Caribbean coast, Mexico

L.M. Hernández-Terrones [a,*,1], J. Street [b], K. Null [b,c], A. Paytan [b]

[a] Universidad del Caribe, L-1. Mz 1, Esq. Fracc. Tabachines SM 78, Cancun, Quintana Roo, 77528, Mexico
[b] Institute of Marine Sciences, University of California Santa Cruz, 1156 High Street, Santa Cruz, CA, 95064, USA
[c] Moss Landing Marine Laboratories, Moss Landing, CA, 95039, USA

ARTICLE INFO

Keywords:
Strontium isotopes
Karst aquifer
Groundwater
Mexican Caribbean
Water-rock interactions
Submarine groundwater discharge

ABSTRACT

Radiogenic strontium isotopic ratios ($^{87}Sr/^{86}Sr$) and solute concentrations in groundwater samples from the coastal area of the eastern Yucatán Peninsula, Quintana Roo, Mexico were measured to assess connectivity and water-rock interactions within different groundwater systems in the region. The average $^{87}Sr/^{86}Sr$ ratios vary from south to north with values in Xcalak around 0.70889, Sian Ka'an around 0.70847 and at Cancun and Puerto Morelos around 0.70880. The values show 3 clusters suggesting 3 distinct groundwater systems, Cancun-Puerto Morelos in the north, Tulum-Sian Ka'an in the center and Xcalak in the South. Water-rock interactions, while unique within each aquifer system, encompass processes observed throughout the Yucatan karst system including dissolution of evaporites, precipitation of carbonate, sulfate reduction and mixing with seawater. This study highlights the use of groundwater chemistry of understanding groundwater connectivity and the importance of potential distal anthropogenic impacts on groundwater quality and related effect on coastal population and ecosystems.

1. Introduction

Strontium (Sr) isotope ratios are increasingly applied to studies of earth surface processes, including delineating water-rock interactions and many other hydro-geochemical applications (Blum and Erel, 2005; Négrel and Petelet-Giraud, 2005; Vengosh et al., 2002). The radiogenic Sr isotope ratio, $^{87}Sr/^{86}Sr$, in soil, groundwater, vegetation, and fauna largely reflect underlying bedrock $^{87}Sr/^{86}Sr$ values, with little contribution from atmospheric sources (Clow et al., 1997; Graustein 1989). Groundwater $^{87}Sr/^{86}Sr$ ratios may be impacted by water-rock interactions in the aquifer, and have been used as tracers for various hydro-geochemical processes, e.g., to identify recharge sources, to constrain water end-members contributing to an aquifer, and to elucidate flow pathways and mixing processes in groundwater systems (Pu et al., 2012; Shand et al., 2009; Négrel and Petelet-Giraud 2005; Barbieri and Morotti, 2003; Capo et al., 1998; Katz and Bullen, 1996). Holmden et al. (2012) and Rahaman and Singh (2012) suggest that major elements such as Ca and Sr and their isotopes may mix non-conservatively in the subterranean estuary mixing zone, highlighting the importance of this interface to submarine groundwater discharge (SGD)-driven chemical fluxes, particularly in carbonate environments. Beck et al. (2013) established that SGD (both fresh and brackish) is an important source of Sr to the modern ocean with large site-specific variability and a global average radiogenic $^{87}Sr/^{86}Sr$ ratio slightly lower than present-day seawater (but see Basu et al., 2001 and Chakrabarti et al., 2018).

The $^{87}Sr/^{86}Sr$ ratio of seawater has increased during the Cenozoic from 0.7074 in the late Cretaceous to 0.7092 for modern seawater (Hodell et al., 2004; McArthur et al., 2000). The radiogenic strontium isotope ratio of marine carbonates reflects the $^{87}Sr/^{86}Sr$ composition of seawater at the time of formation (any mass dependent fractionation is corrected during isotope analysis due to normalization to constant $^{86}Sr/^{88}Sr$ of 0.1194). Because calcite and aragonite have a low Rb/Sr ratio most marine carbonates accumulate insignificant radiogenic ^{87}Sr

* Corresponding author.
E-mail address: lmhernandez@ucaribe.edu.mx (L.M. Hernández-Terrones).
[1] Former address: Centro de Investigación Científica de Yucatán, Unidad de Ciencias del Agua, Calle 8 #39, L-1, Mz 29, SM 64, 77524, Cancun, Quintana Roo, México.

https://doi.org/10.1016/j.csr.2020.104293
Received 6 December 2019; Received in revised form 30 October 2020; Accepted 2 November 2020
Available online 9 November 2020

from ^{87}Rb decay over time, conserving original seawater Sr isotope signatures (McArthur et al., 2000). Hence groundwater interacting with carbonate rocks of distinct ages tend to have unique isotopic signatures reflecting the seawater value at the time of formation of the aquifer bedrock as modified by post burial diagenesis.

In the Yucatán Peninsula, Sr concentrations and isotope ratios in groundwater have proven to be reliable indicators of groundwater interactions with limestone and evaporitic deposits (Perry et al., 2002). However, little work has been done in the eastern Yucatán Peninsula in the state of Quintana Roo (Perry et al., 2009). Only one significant surface stream (Río Hondo in southern Quintana Roo) flows in this region and rainfall readily percolates through the underlying limestone until it reaches the aquifer where it flows towards the coast (Bauer--Gottwein et al., 2011). Seawater intrusion is common along the coast in this region and mixing between groundwater and seawater within the aquifer is prevalent (Perry et al., 2002). As a result, the $^{87}Sr/^{86}Sr$ of groundwater in the Yucatán Peninsula is expected to reflect the signature of the aquifer bedrock due to dissolution or exchange of Sr through water-rock interactions, as well as any mixing with present day seawater in the coastal aquifers. This is because Sr concentrations in carbonates are high compared to those in rainwater or those leached from the very thin soil layer in this region. Water-rock interactions that affect groundwater chemistry throughout the Yucatan Peninsula include dissolution of evaporites (increasing Sr^{2+} and SO_4^{2-} relative to seawater); precipitation of carbonate within the aquifer which will removes some of the added Sr^{2+}, and sulfate reduction a process that removes much of the SO_4^{2-} (Perry et al., 2002, 2009). The aim of this study was to use radiogenic Sr isotope ratios and groundwater chemistry in samples collected along the Quintana Roo coast of the Yucatán Peninsula to characterize coastal groundwater systems along the Mexican Caribbean for which only limited data exists (Perry et al., 2009; Hodell et al., 2004; Null et al., 2014). We compare data from three different geomorphological regions (Cancun-Puerto Morelos, Sian Ka'an and Xcalak) to assess their connectivity. The data and conclusions from this work are particularly important given the sensitivity of groundwater to anthropogenic impacts in karst systems and the importance of groundwater the coastal communities and ecosystem.

2. Study area

2.1. Groundwater and development in the Yucatan

Water samples for this study were collected in three regions along the coast in the state of Quintana Roo (QR), Cancun-Puerto Morelos, Sian Ka'an, and Xcalak (Fig. 1). The Mexican Caribbean coast is facing increasing development, population and tourism growth, resulting in increased pressure on water resources. Groundwater flow regimes have important implications for development in the Yucatan Peninsula. Tourism on the Mexican Caribbean coast has dramatically increased in the last decade (from ~8,000,000 tourists in 2008 to more than 15, 000, 000 in 2015; Secretaría de Turismo de Quintana Roo, 2015 sedetur.qroo.gob.mx) with related increase in coastal infrastructure and associated demand for services. Since most of the precipitation infiltrates in the subsurface, groundwater is the only freshwater source for this region with a freshwater lens thickness of ~10 m (near the coast) to 100 m (inland) depending on location (Gondwe et al., 2010). There is already evidence of elevated nitrate concentrations in groundwater in Quintana Roo (Hernández-Terrones et al., 2011; 2015; Herrera-Silveira et al., 2009; Mutchler et al., 2007), hence it is necessary to understand the spatial structure and the connectivity of groundwater in this area to prevent impacts of future development and associated anthropogenic pollutants on water quality and availability to coastal communities and valuable coastal ecosystems. Each of the sites we selected for sampling has different urban development infrastructure and hosts a different number of tourists and hence the sites represent a gradient in human impacts. Cancun is a major tourist destination with >7 million tourists each year. Puerto Morelos a small coastal fishing village located ~35 km south of Cancun offers 5072 accommodations for tourism. The area between Cancun and Puerto Morelos is heavily developed and lined by many tourist resorts and hotels. The Cancun and Puerto Morelos results were combined into one group because of their close geographic position (Table 1). Sian Ka'an, a biosphere reserve, is located ~120 km south of Cancun, it is dominated by tropical forests and mangroves in the Tulum municipality with just 7082 accommodations. The town of Xcalak, with 375 residents in the southernmost part of our study area (240 km south of Tulum), and the national marine park in Xcalak, attract relatively few tourists (INEGI, 2017).

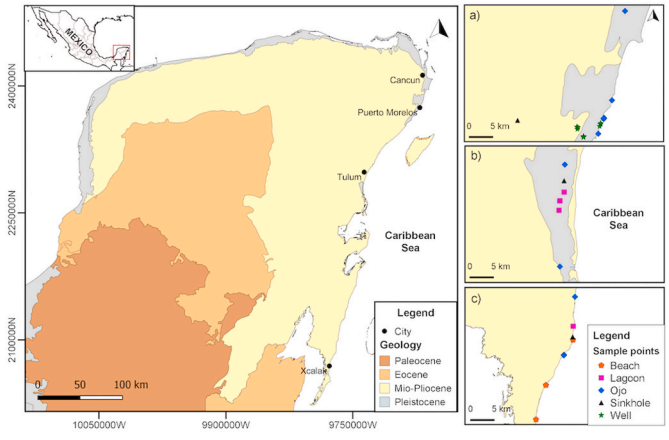

Fig. 1. Study sites location map, a) Cancun-Puerto Morelos, b) Sian Ka'an, c) Xcalak. Geological map reference: SGM (2007).

2.2. Groundwater systems at the Caribbean cast of Quintana Roo

The Yucatán Peninsula is a large carbonate platform composed of rocks ranging from Cretaceous to Quaternary in age (Gilli et al., 2009). Hodell et al. (2004) analyzed $^{87}Sr/^{86}Sr$ of water, bedrock, soils, and plants throughout the Yucatan Peninsula and identified five distinct regions based on the Sr isotopes. Specifically, Cancun, Puerto Morelos and Sian Ka'an were all included in the Northern Lowland zone (with $^{87}Sr/^{86}Sr$ of 0.70888 ± 0.00066) while Xcalak was located in the Southern Lowlands (with $^{87}Sr/^{86}Sr$ 0.70770 ± 0.00052). Based on these data and groundwater flow paths derived from hydrological and geophysical data as summarized in Bauer-Gottwein et al. (2011) our four sampling regions were expected to represent two groundwater systems. Based on geological mapping, Cancun, Puerto Morelos, and Sian Ka'an are located in the Holbox/Xel Ha Fracture Zone, whereas Xcalak is located in the "Evaporite Region" (Perry et al., 2002). Perry et al. (2002) reported on the groundwater systems in the region, however, they did not include samples from the northern area of QR and recommended that this region should be further investigated. We note however that surface mapping and even bedrock chemistry may not reflect groundwater connectivity in karst settings; hence chemical signatures of groundwater and nearshore water may shed more light on subsurface water flow. Specifically, Null et al. (2014) based on Ra isotope ratios in water samples (the ratios of the four Ra isotopes can serve to distinct between aquifers because there ratios depend on the U–Th ratios of the aquifer rocks and the residence time of groundwater in the aquifer, Moore, 1999) collected at the same four regions we sampled concluded that these sites represent three distinct water systems, Cancun-Puerto Morelos in the north, Tulum-Sian Ka'an in the center and Xcalak in the south, rather than two.

Table 1
Sampling sites coordinates and field excursions dates.

Location	Site	Coordinates		Date
		Latitude	Longitude	
Cancun/Puerto Morelos	Ojo 1	21.093360	−86.815690	January 2009
	Ojo 2	20.881150	−86.860210	January 2009
	Ojo 3	20.916170	−86.843480	January 2009
	Ojo 4	20.849780	−86.872540	April 2008
	Ojo 5	20.879230	−86.860920	April 2008
	Ojo 6	20.880200	−86.861340	April 2008
	Well 1	20.868500	−86.867590	April 2008
	Well 2	20.863460	−86.918010	April 2008
	Well 3	20.859040	−86.916890	April 2008
	Well 4	20.862260	−86.915750	April 2008
	Well 5	20.844560	−86.903860	April 2008
	Well 6	20.842950	−86.903970	April 2008
	Well 7	20.864590	−86.869580	April 2008
	Well 8	20.870410	−86.867690	April 2008
	Sinkhole	20.876340	−87.043950	April 2008
Sian Ka'an	Lagoon 1	20.070480	−87.487530	October 2009
	Lagoon 2	20.063180	−87.491330	October 2009
	Lagoon 3	20.055260	−87.492140	October 2009
	Ojo 1	20.093660	−87.486910	October 2009
	Ojo 2	20.007960	−87.491330	October 2009
	Sinkhole	20.080090	−87.487560	October 2009
Xcalak	Beach 1	18.335917	−87.816117	January 2009
	Beach 2	18.335917	−87.816100	January 2009
	Beach 3	18.417430	−87.764550	January 2009
	Beach 4	18.274190	87.834820	January 2009
	Ojo 1	18.390680	87.781790	January 2009
	Ojo 2	18.389660	87.782020	January 2009
	Ojo 3	18.494980	87.760780	January 2009
	Sinkhole	18.422900	87.765190	January 2009
	Lagoon 1	18.441967	87.764250	January 2009

3. Materials and methods

3.1. Sample collection and analysis

Water samples were collected during four field excursions between April 2008 and October 2009 (Table 1). Importantly, despite collection in different years all sampling was done during the dry season (October–May) to avoid any dilution by fast percolation of rainwater. Samples at each site were collected from the coastal zone, including reef-lagoon surface water (nearshore), beach groundwater from the coastal shallow unconfined aquifer (obtained from shallow pits of 0.5–2 m depth located immediately above the high tide line (where possible these samples were collected along a transect from the tide line inland), coastal offshore submarine springs (locally called "ojos"), inland groundwater (from wells and sinkholes) and surface water from inland lagoons (Fig. 1).

The water samples were collected at each site using submersible pumps. Samples were filtered in the field (0.45 μm), collected in Nalgene® bottles (acid-cleaned, rinsed with MilliQ® water and with sample water), acidified (with trace metal grade HCl to pH < 2) and transported in coolers to the laboratory for analysis. Samples from ojos were collected by scuba divers at each sampling location. Samples from all sites were analyzed for the concentrations of dissolved Sr^{2+}, SO_4^{2-}, Cl^-, and for strontium isotopes ($^{87}Sr/^{86}Sr$). Other water parameters (salinity, pH, temperature) were measured in the field using a calibrated hydrolab DS5 datasonde (HACH). The precision of the data for each sensor was as follows: temperature ±0.10 °C; conductance ±0.001 mS/cm; pH ± 0.2 units; and salinity ±0.2.

3.2. Strontium concentration and isotope ratio analyses

$^{87}Sr/^{86}Sr$ ratios were determined on a ThermoFinnigan Neptune multicollector inductively coupled plasma mass spectrometer (MC-ICP-MS) at the University of California Santa Cruz. For Sr isotope analysis a fraction of each water sample representing ~1 μg Sr was evaporated to dryness, re-dissolved in 3 M distilled HNO_3, and passed through 2 mL columns containing pre-cleaned, preconditioned Sr-SpecTM resin (EiChrom Technologies, bead size of 50–100 μm). After several washes with 3 M HNO_3, Sr was eluted in ultrapure deionized water and the collected aliquot dried, then re-dissolved in 3% HNO_3 for MC-ICP-MS analysis. The data were externally corrected to SRM 987 (strontium carbonate isotope standard dissolved in 3% HNO_3; $^{87}Sr/^{86}Sr = 0.710248$), which was run concurrently with the samples. The external, measured 2σ reproducibility of the SRM 987 was ±0.00006 ($n = 45$). Blanks were processed with each batch of samples. Strontium concentrations were analyzed by ICP-OES (Iris Intrepid II, Thermo-Electron Corp). Strontium TraceCert Sigma-Aldrich standard was used for calibration. The analyses were done at the Water Sciences Unit of Centro de Investigación Científica de Yucatán. Samples, standards and blanks were prepared for samples analyses with ultrapure deionized water.

3.3. Sulfate and chloride analyses

Sulfate and chloride analyses were conducted according to the methods described in Standard Methods for the Examination of Water and Wastewater (APHA 1998), at the Water Sciences Unit of CICY. In short, the turbidimetric method for sulfate and the argentometric method for chloride were used. The uncertainty for these analyses was ±0.69% for sulfate and ±0.30% for chloride.

4. Results and discussion

The concentrations of Sr^{2+}, SO_4^{2-}, Cl^-, salinity and the $^{87}Sr/^{86}Sr$ ratio of different sample types at each of the sites are given in Table 2. Overall, the $^{87}Sr/^{86}Sr$ ratios differed between sites and between water types within each site (Table 2). Sr^{2+} concentrations in all samples were lower than or similar to the seawater concentration (92 μM) (Table 2). When plotting Sr^{2+} vs. Cl^- or Sr^{2+} vs SO_4^{2-} (Figs. 2–4) a few samples plot slightly above the line corresponding to the seawater ratios (e.g., a mixing line with end member concentrations representing seawater and solute free freshwater at the origin) and most samples plot below the seawater ratio. SO_4^{2-} concentrations were lower than those of seawater (28.94 mM for salinity of 35; Pilson, 2013) for most samples (0.04–25.96 mM) but a few samples had concentrations that were similar to seawater (Table 2). Concentrations of dissolved SO_4^{2-} and Cl^- for each site are presented in Figs. 2–4. The samples show a wide range of SO_4^{2-}/Cl^- molar ratios (0.01–0.92), with ratios lower and higher than the seawater ratio (0.05; Pilson, 2013).

The relationship between Sr isotope ratios and the molar ratio of 1000*Sr/Cl at the different sites (Figs. 2–4) is used to assess seawater intrusion and the presence of evaporites (Perry et al., 2002). Specifically, Sr^{2+}/Cl^- ratios approaching the seawater and Sr isotopes around 0.7092 are consistent with seawater intrusion, while Sr^{2+}/Cl^- ratios higher than those of seawater and less radiogenic Sr isotopes are consistent with the input from the dissolution of older (Eocene)

Table 2
Sampling sites and data for the $^{87}Sr/^{86}Sr$, salinity, SO_4^{2-}, Cl^-, and $1/Sr^{2+}$.

Location	Site	$^{87}Sr/^{86}Sr$	$1/[Sr^{2+}]$	$[Cl^-]$	$[Sr^{2+}]$	$[SO_4^{2-}]$	Salinity
		Normalized		mM	μM	mM	
Cancun/Puerto Morelos	Ojo 1	0.70916	8.93	26.52	112	24.32	26.40
	Ojo 2	0.70896	12.82	600.36	78	25.08	28.37
	Ojo 3	0.70885	43.48	451.85	23	13.40	25.28
	Ojo 4	0.70800	500	619.32	2	15.07	32.40
	Ojo 5	0.70924	22.73	655.66	44	25.96	26.60
	Ojo 6	0.70863	200	538.75	5	15.81	29.00
	Well 1	0.70896	125	44.05	8	1.40	2.6
	Well 2	0.70909	16.39	8.47	61	0.70	0.30
	Well 3	0.70912	50	3.88	20	0.11	0.50
	Well 4	0.70918	100	2.33	10	0.04	0.50
	Well 5	0.70923	29.41	4.73	34	0.11	0.60
	Well 6	0.70912	19.61	4.45	51	0.13	1.00
	Well 7	0.70909	9.35	78.81	107	1.86	5.10
	Well 8	0.70911	11.90	59.04	84	1.71	4.30
	Sinkhole	0.70849	90.91	43.64	11	0.46	0.70
Sian Ka'an	Lagoon 1	0.70862	17.86	301.15	56	12.39	18.57
	Lagoon 2	0.70876	23.26	312.1	43	13.88	17.00
	Lagoon 3	0.70857	21.74	306.62	46	11.50	18.99
	Ojo 1	0.70829	125	7.71	8	0.35	0.59
	Ojo 2	0.70809	16.12	314.84	62	15.00	13.60
	Sinkhole	0.70859	32.26	306.62	31	11.50	13.83
Xcalak	Beach 1	0.70914	76.92	15.27	13	1.99	1.60
	Beach 2	0.70804	58.82	38.19	17	2.93	2.34
	Beach 3	0.70902	58.82	379.18	17	16.41	20.65
	Beach 4	0.70899	111.11	44.99	9	3.61	1.08
	Ojo 1	0.70913	37.04	603.52	27	17.38	14.30
	Ojo 2	0.70867	35.71	271.74	28	13.10	22.96
	Ojo 3	0.70904	29.41	660.4	34	30.50	15.07
	Sinkhole	0.70869	21.74	468.94	46	22.13	27.28
	Lagoon 1	0.70914	66.67	74.75	15	3.68	6.20

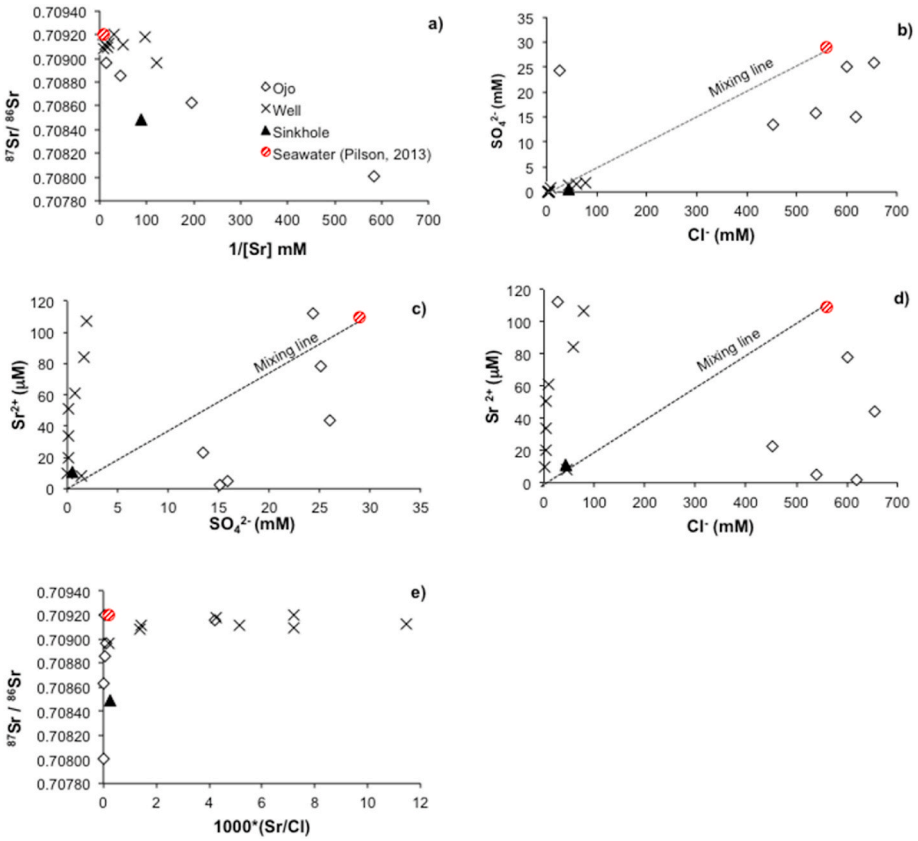

Fig. 2. Cancun-Puerto Morelos: a) $^{87}Sr/^{86}Sr$ ratio vs. $1/[Sr^{2+}]$, b) SO_4^{2-} (mM) vs. Cl^- (mM), c) Sr^{2+} (μM) vs. SO_4^{2-} (mM), d) Sr^{2+} (μM) vs. Cl^- (mM) concentrations, e) $^{87}Sr/^{86}Sr$ ratio vs 1000*(Sr/Cl), for different sample types (beach groundwater, lagoon, ojo, well, sinkhole). Concentrations and ratios for seawater are shown in red, and mixing is shown as dashed line. (For interpretation of the references to colour in this figure legend, the reader is referred to the Web version of this article.)

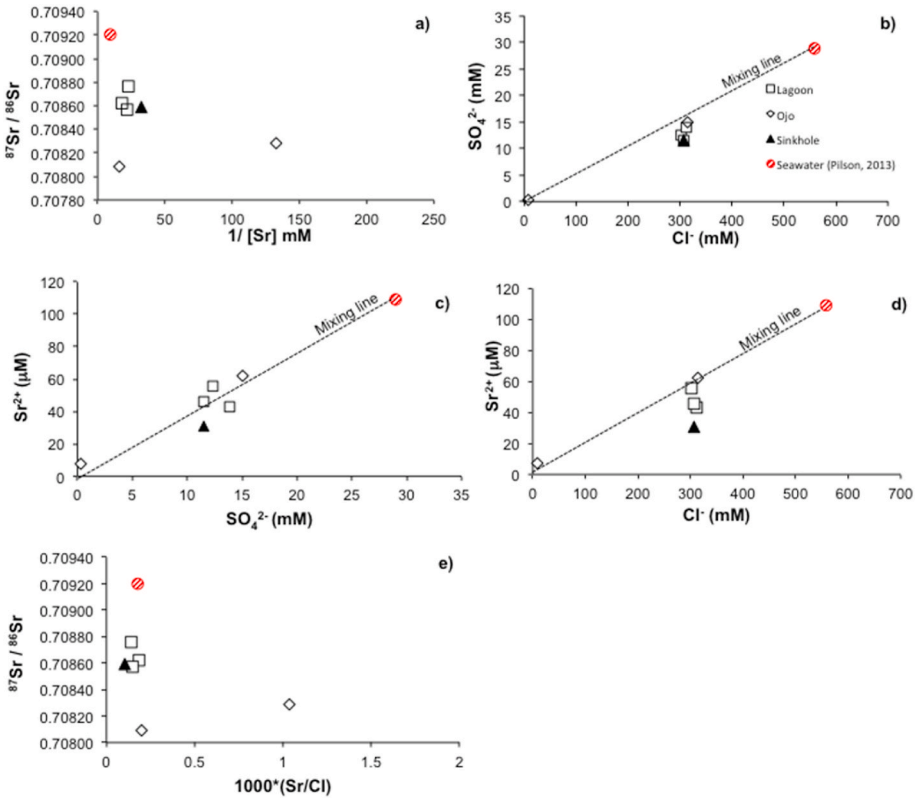

Fig. 3. Sian Ka'an: a) $^{87}Sr/^{86}Sr$ ratio vs. $1/[Sr^{2+}]$, b) SO_4^{2-} (mM) vs. Cl^- (mM), c) Sr^{2+} (µM) vs. SO_4^{2-} (mM), d) Sr^{2+} (µM) vs. Cl^- (mM) concentrations, e) $^{87}Sr/^{86}Sr$ ratio vs 1000*(Sr/Cl), for different sample types (beach groundwater, lagoon, ojo, well, sinkhole). The seawater data is marked in red and mixing is shown as dashed line. (For interpretation of the references to colour in this figure legend, the reader is referred to the Web version of this article.)

evaporites in this region.

Table 3 shows the mean values and SD (standard deviation) of different parameters in the studied sites and between geological units within each site. In general, the $^{87}Sr/^{86}Sr$ ratios in surface waters from brackish lagoons and sinkholes were less radiogenic than present day seawater values and differed between geological units (average of 0.70900 for the lagoons and 0.70864, for the sinkholes) but there was no consistent trend with distance from shore at each site (Table 3). The results show an increasing trend from Cancun/Puerto Morelos to Xcalak is salinity, SO_4^{2-}, and Cl^- average concentrations, the trend was less evident between geological units (Table 3).

The $^{87}Sr/^{86}Sr$ signature of the ojos in Puerto Morelos-Cancun (north sites) is slightly more radiogenic than the ratios of the Sian Ka'an groundwater samples indicating interaction with rocks and minerals of distinct ages (younger rocks in the north compared to the south) and hence indicating unique aquifer systems, although both corresponds to rocks of Miocene-Pleistocene age. This is consistent with radium (Ra) isotope data reported by Null et al. (2014) but in contrast to the grouping by Hodell et al. (2004) or Bauer-Gottwein et al. (2011). Indeed, Gondwe et al. (2010) suggested that Sian Ka'an is located in the Rio Hondo fracture zone that intersects the Holbox fracture zone near Tulum, and therefore may represent a separate groundwater system, distinct from the aquifers to the north or south. The $^{87}Sr/^{86}Sr$ signatures in Xcalak are more radiogenic than those in Sian Ka'an and are more similar to those of Cancun-Puerto Morelos. The $^{87}Sr/^{86}Sr$ data are consistent with the idea of three unique aquifer systems along the coastal Quintana Roo (Null et al., 2014). Moreover, based on the SO_4^{2-}/Cl^- ratios it seems that the Xcalak coastal aquifer waters differ from the other sites as these samples have higher Sr^{2+}/Cl^- ratios than those of seawater which is consistent with dissolution of evaporites and possibly celestite in this region (see discussion below).

To investigate the specific processes controlling water chemistry withing each of the 3 zones we look in more detail into the data for the various sample types in each area.

4.1. Cancun-Puerto Morelos

The $^{87}Sr/^{86}Sr$ ratios of the coastal pits and some of the well samples from Cancun-Puerto Morelos (0.70896–0.70918) were close to the seawater $^{87}Sr/^{86}Sr$ ratio (0.7092). Other wells had less radiogenic $^{87}Sr/^{86}Sr$, falling between present day seawater values and those of the brackish lagoons and sinkholes (0.7085). The ojos also ranged between seawater and the brackish lagoon and sinkhole values, although one ojo at Puerto Morelos had the lowest $^{87}Sr/^{86}Sr$ signature (0.7080) (Fig. 2a). SO_4^{2-} concentrations at three Puerto Morelos ojos were similar to or lower than seawater. Most samples had Sr^{2+} concentrations lower than the seawater concentration (92 µM; Pilson, 2013), except for one well and one ojo with concentrations slightly higher (107 and 112 µM respectively) than seawater. Well and sinkhole samples had SO_4^{2-}/Sr^{2+} ratios lower than seawater and the ojo samples had SO_4^{2-}/Sr^{2+} ratios higher than seawater, except for one ojo that had high Sr^{2+} and high SO_4^{2-} with excess Sr^{2+} relative to seawater (Fig. 2c). The wells in Cancun-Puerto Morelos have very low Cl^- (2.33–8.47 mM) but variable and higher Sr^{2+} (10–61 µM) relative to Cl^- when compared to the seawater value. The ojo samples present an opposite trend, higher Cl^- (451.85–655.66 mM) relative to Sr^{2+}, except for one ojo with low Cl^- (26.52 mM) and high Sr^{2+} (112 µM), when compared to the seawater ratio. The sinkhole samples were depleted in both Cl^- and Sr^{2+} with ratios that are similar to that of seawater (0.05) (Fig. 2d). Samples of the wells and one ojo had high values of 1000*Sr/Cl, ranging from 4.22 to 11.46. These waters are relatively fresh (all have low chloride relative to seawater concentrations), and Sr isotope ratios close to those of seawater (Fig. 5a). The ojo samples and sinkhole have 1000*Sr/Cl lower than 0.25 and Sr isotope ratios between 0.7090 and 0.7084 (Fig. 2e). Overall, the

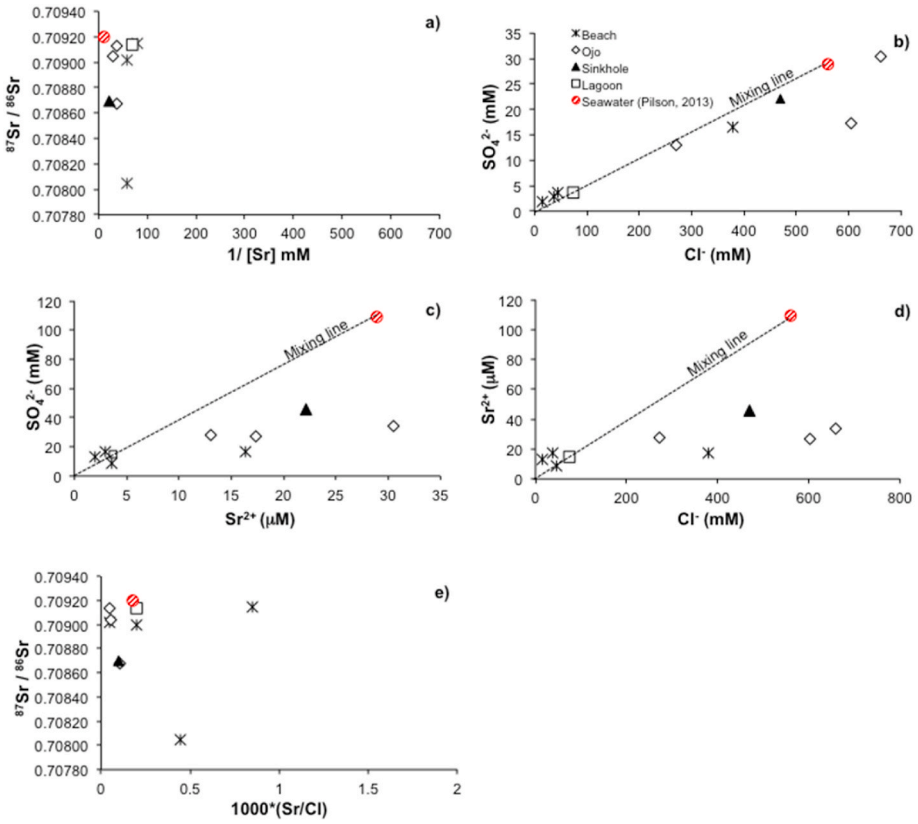

Fig. 4. Xcalak: a) $^{87}Sr/^{86}Sr$ ratio vs. $1/[Sr^{2+}]$, b) SO_4^{2-} (mM) vs. Cl^- (mM), c) Sr^{2+} (µM) vs. SO_4^{2-} (mM), d) Sr^{2+} (µM) vs. Cl^- (mM) concentrations, e) $^{87}Sr/^{86}Sr$ ratio vs 1000*(Sr/Cl), for different sample types (beach groundwater, lagoon, ojo, well, sinkhole). Seawater data is plotted in red and mixing is shown as dashed line. (For interpretation of the references to colour in this figure legend, the reader is referred to the Web version of this article.)

samples from Cancun-Puerto Morelos fall into three groups one containing the wells and sinkhole, a second containing most of the ojos and a third that is represented by one unique ojo sample (Fig. 2).

The $^{87}Sr/^{86}Sr$ ratios of the Puerto Morelos wells within 20 km of the shoreline are close to the present-day seawater signature (0.7092) despite low salinity (<7), likely reflecting the interaction of meteoric groundwater with rocks in the coastal aquifer and the dissolution of carbonates that are of relatively young (<2 Ma) (Hodell et al., 2004; Paytan et al., 1993; Veizer et al., 1989). The high Sr^{2+} concentrations (normalized to Cl^-) in the freshwater wells is also consistent with dissolution of young Sr^{2+} rich carbonate rocks. In contrast, the ojo samples of Cancun-Puerto Morelos span a wide range in $^{87}Sr/^{86}Sr$ ratios from around the present-day seawater value (0.7092) to as low as 0.70800, suggesting that these samples reflect contributions from a distinct groundwater source, a deeper aquifer that experiences interaction with rocks of Miocene-Pleistocene age, which are characterized by $^{87}Sr/^{86}Sr$ ratios that are lower than present-day seawater and various degrees of mixing with seawater. Most samples from Cancun-Puerto Morelos also have SO_4^{2-}/Cl^- ratios equal or lower than the seawater ratio, suggesting varying degrees of SO_4^{2-} reduction within the aquifer. SO_4^{2-} reduction is prevalent in aquifers that have become anoxic due to long water residence times or high organic matter content. According to Perry et al. (2002), in sites where the fresh water lens is near the surface (i.e. near the coast), plant roots supply organic matter that supports SO_4^{2-} reduction; many of the samples we analyzed are from locations relatively close to the shoreline. The sinkhole and two well samples representing the deeper aquifer have low SO_4^{2-} and low Sr^{2+} concentrations when normalized to seawater, suggesting that in addition to SO_4^{2-} reduction carbonate is precipitating in the aquifer. None of the samples had high Sr^{2+} when normalized to Cl^-, except for one ojo that also had a high SO_4^{2-}/Cl^- ratio which may be attributable to evaporite dissolution. The low Sr^{2+} concentrations relative to Cl^- in these samples (except for the one ojo) suggest carbonate precipitation in the aquifer and that this precipitation is more important than evaporite dissolution in controlling the water chemistry in this aquifer.

4.2. Sian Ka'an

The $^{87}Sr/^{86}Sr$ in lagoons and sinkholes at Sian Ka'an ranged between 0.70859 and 0.70876. The ojos had less radiogenic $^{87}Sr/^{86}Sr$ signatures (Fig. 3a). The SO_4^{2-} and Cl^- concentrations and the SO_4^{2-}/Cl^- ratio were lower than those of seawater for all samples (Fig. 3b). All sample types from Sian Ka'an also had Sr^{2+} and SO_4^{2-} concentrations lower than seawater but Sr^{2+}/SO_4^{2-} ratios similar or slightly lower (for the sinkhole) than to those of seawater (Fig. 3c). Fig. 3d show the that Sr^{2+} and Cl^- concentrations for all the samples were lower than those of seawater with the sinkhole and lagoon samples plotting below the seawater ratio and the ojo samples have ratios close to that of seawater. All but one ojo sample has 1000*Sr/Cl ratios lower than 0.5 (Fig. 3e).

The SO_4^{2-}/Cl^- ratios for this site which are close to the seawater value (0.05) indicate limited sulfate reduction in the aquifer. The low $^{87}Sr/^{86}Sr$ ratios, along with low Sr^{2+} concentrations (normalized to Cl^-) suggest complex chemical interactions in the aquifer involving dissolution of evaporite and carbonate minerals that contribute less radiogenic Sr^{2+} and re-precipitation of this Sr^{2+} as secondary carbonates within the aquifer. This variable mixing results in variable $^{87}Sr/^{86}Sr$ signature of the ojos, sinkhole and the lagoons, which receive substantial groundwater input. Aquifer rocks with low Sr^{2+} concentrations and less radiogenic $^{87}Sr/^{86}Sr$ ratios compared to present-day seawater suggest Cretaceous or older Cenozoic carbonate and/or evaporite rocks dissolved to release Sr^{2+} to the groundwater. In the coastal shallow aquifer, the water chemistry is indicative of mixing between seawater and a

Table 3
Mean values and SD (standard deviation) of different parameters in the studied sites and between geological units.

Site	$^{87}Sr/^{86}Sr$						
	Normalized						
	Well	Sinkhole	Lagoon	Beach	Ojo	Average	SD
Cancun/Puerto Morelos	0.70911	0.70849			0.70880	**0.70880**	0.0003
Sian Ka'an		0.70859	0.70864		0.70819	**0.70847**	0.0002
Xcalak		0.70869	0.70914	0.70879	0.70894	**0.70889**	0.0002
Average		**0.70864**	**0.70900**		**0.70859**		
SD		0.0004	0.0002		0.0003		
Site	**$1/[Sr^{2+}]$**						
	Well	Sinkhole	Lagoon	Beach	Ojo	**Average**	**SD**
Cancun/Puerto Morelos	45.21	90.91			131.33	**89.15**	43.09
Sian Ka'an		32.26	20.95		70.56	**41.26**	26.00
Xcalak		21.74	66.67	76.42	34.05	**49.72**	26.00
Average		**48.30**	**43.81**		**78.65**		
SD		37.27	32.33		49.14		
Site	**$[Cl^-]$ mM**						
	Well	Sinkhole	Lagoon	Beach	Ojo	Average	SD
Cancun/Puerto Morelos	25.72	43.64			482.07	**183.81**	258.46
Sian Ka'an		306.62	306.62		161.28	**258.17**	83.91
Xcalak		468.94	74.75	119.41	511.89	**293.75**	240.94
Average		**273.07**	**190.69**		**385.08**		
SD		214.63	163.96		194.39		
Site	**$[Sr^{2+}]$ µM**						
	Well	Sinkhole	Lagoon	Beach	Ojo	Average	SD
Cancun/Puerto Morelos	46.88	11.00			44.00	**33.96**	19.94
Sian Ka'an		30.81	48.33		35.00	**38.05**	9.15
Xcalak		45.54	14.61	13.81	27.50	**25.37**	14.84
Average		**29.12**	**31.47**		**35.5**		
SD		*17.33*	*23.84*		*8.26*		
Site	**$[SO_4^{2-}]$ mM**						
	Well	Sinkhole	Lagoon	Beach	Ojo	Average	SD
Cancun/Puerto Morelos	0.75	0.46			19.94	**7.05**	11.16
Sian Ka'an		11.5	12.6		7.68	**10.59**	2.58
Xcalak		22.13	3.68	6.24	15.20	**11.81**	8.47
Average		**11.36**	**8.14**		**14.27**		
SD		10.84	6.31		6.18		
Site	**Salinity**						
	Well	Sinkhole	Lagoon	Beach	Ojo	**Average**	SD
Cancun/Puerto Morelos	1.86	0.70			28.01	**10.19**	15.44
Sian Ka'an		13.83	18.19		7.10	**13.04**	5.59
Xcalak		27.28	6.2	6.42	17.44	**14.34**	10.10
Average		**13.94**	**12.19**		17.52		
SD		13.29	8.48		10.46		

relatively fresh groundwater source with a low $^{87}Sr/^{86}Sr$ signature. Higher Sr^{2+} and more radiogenic Sr isotopes closer to the coast are consistent with a higher contribution of seawater closer to shore. However, many samples had lower Sr^{2+} concentrations than expected from simple mixing between the groundwater and seawater endmembers, indicating some Sr^{2+} loss due to precipitation of carbonate upon interaction with seawater resulting from the nonlinear dependence of $CaCO_3$ saturation on salinity (Singurindi et al., 2004; Perry et al., 1989).

4.3. Xcalak

In Xcalak, the $^{87}Sr/^{86}Sr$ ratio for beach groundwater ranged between 0.70804 and 0.70914, with the ratio for some samples close to the seawater signature. The lagoon $^{87}Sr/^{86}Sr$ ratio was similar to that of seawater, the sinkhole had a less radiogenic value of 0.7087. Ojo samples had ratios that were lower than seawater (0.70867–0.70913) and were equal or lower Sr^{2+}/Cl^- ratios than the seawater Sr^{2+}/Cl^- ratio. The beach and lagoon samples had low Cl^- (15.27–74.75 mM) and Sr^{2+} (9–17 µM) concentrations (Fig. 4d) but had similar or slightly higher SO_4^{2-}/Cl^- ratios than seawater (Fig. 4b). The samples at Xcalak were distributed in two groups, the beach sites cluster in the group at or above the seawater SO_4^{2-}/Cl^- ratio, and the lagoon, ojos and sinkhole have higher SO_4^{2-} and Cl^- concentrations and ratios that fall below those of seawater (with the exception of one ojo that was more similar to seawater in concentrations and ratios) (Fig. 4b). All Xcalak samples had low SO_4^{2-}/Sr^{2+} ratios relative to seawater (Fig. 4c). All but one sample had 1000*Sr/Cl ratios lower than 0.5 (Fig. 4e).

The range of $^{87}Sr/^{86}Sr$ ratios in Xcalak was small, all ratios are close to 0.7090, representative of young carbonate rocks. Specifically, the shallow fresh groundwater lens (represented by the beach samples) seems to have equilibrated with local aquifer carbonate rocks, which have ratios close to 0.7090 (young carbonate deposits) (Hodell et al., 2004). The SO_4^{2-}/Cl^- ratios that are higher than seawater likely reflect a contribution of sulfate from gypsum/anhydride dissolution in some beach sites (Fig. 4b). Aquifer rocks around Xcalak include gypsum and or anhydride, or possibly celestite. Previous geochemical studies

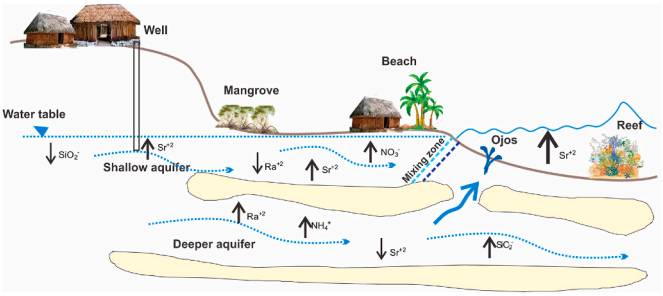

Fig. 5. Characteristics of the conceptual model of the coastal aquifer at sampling sites, showing 3 distinct systems and a shallow and deeper aquifer for each one (Ra data from Null et al., 2014; nutrients data from Hernández-Terrones et al., 2011). The arrows indicate higher (↑) or lower (↓) values for the parameters. The arrow thickness represents differences in concentration.

performed by Perry et al. (2009) indicate that the evaporite distribution in the region is related to the location of Paleocene and Eocene rocks. Tobón-Velázquez et al. (2018), recently showed high Sr concentrations in Bacalar Lagoon, inferring that this could be due to evaporites dissolution. Indeed, these samples may reflect interaction with aquifers where the rocks are similar to the gypsum quarries in this area that correspond to the evaporitic Icaiche formation (Lopez-Ramos, 1975) and represent a distinct aquifer.

The groundwater geochemistry in the aquifers samples along the QR coast is determined by 4 co-occurring processes that impact the groundwater at different rates. The first three reflect water-rock interactions withing the aquifer (1) dissolution of evaporites (increasing Sr and SO_4^{2-} relative to seawater); (2) precipitation of carbonate that removes some of the added Sr^{2+}; (3) sulfate reduction that removes much of the sulfate; and the fourth represents (4) mixing with seawater to various degrees (Fig. 5). Sr isotopes reflect interactions with rocks of different ages. Interestingly, none of the samples in our study fall directly along the Sr^{2+}/SO_4^{2-} relationship showed by Perry et al. (2002), this may indicate that differences in processes occurring within a region between coastal (our data) and more inland sites (samples by Perry et al., 2002). The studied sites we describe all have a distinct shallow aquifer system that has different characteristics than the deeper aquifer at the corresponding sites (represented by the shallow wells of Cancun-Puerto Morelos, and beach groundwater samples from Xcalak) (Hernández-Terrones et al., 2011).

5. Conclusions

The geochemical signatures of the analyzed water samples reflect the chemical changes that occur in the aquifers through water-rock interaction (dissolution or precipitation of anhydride/gypsum and carbonate) and sulfate reduction (Jones et al., 1999), as well as varying degrees of mixing with seawater. A combination of all of these processes is seen in the various aquifers and based on the occurrence of these processes in distinct locations and sample type; it is possible to distinguish between different aquifers. Specifically, along the coast of Quintana Roo we identify three distinct aquifer systems (Cancun-Puerto Morelos, Sian Ka'an, and Xcalak), and within each of these systems the unconfined aquifer is distinct from the deeper aquifers. Hodell et al. (2004) analyzed water from 25 sampling sites along the Yucatan and Quintana Roo and they report a continuous progression of Sr^{2+} exchange of groundwater with older rocks as the water moves along the subsurface flow path from south to north, suggesting one connected aquifer in which groundwater chemistry changes along the flow path with time. However, in this study, which is confined to the coastal area, no such trend was observed, and the results suggest different and distinct aquifers, a conclusion consistent with previously published Ra data (Null et al., 2014). Our results demonstrate that the combination of Sr isotopes along with the Sr^{2+}, SO_4^{2-} and Cl^- concentrations are sensitive tracers of groundwater sources and rock water interactions in the eastern part of the Yucatán Peninsula, as highlighted before by Perry et al. (2002) for other regions in the Yucatán. Moreover, these results stress the need to understand the connectivity of aquifer systems to prevent impacts of future development, water pressure and climate change on groundwater quality. To understand the connectivity can help to prevent groundwater pollution, and the potential impact of inland anthropogenic activities on coastal coral reefs and other ecosystems.

Declaration of competing interest

The authors declare that they have no known competing financial interests or personal relationships that could have appeared to influence the work reported in this paper.

Acknowledgments

We would like to thank the UCMexus-CONACYT grant and the CONACYT CB-134843 grant, for funding. We extend many thanks to PNAPM-CONANP Marine Park for their support, to Nidia Tobón Velázquez for help with Fig. 5, to Juan Carlos Zamora Luria, and to people in the Paytan Lab at UCSC for field and laboratory assistance. We are also thankful to Rosa Ma. Loreto for her valuable help during fieldwork.

References

American Public Health Association (APHA), 1998. In: Eaton, A.D., Clesceri, L.S., Greenberg, A.E. (Eds.), Standard Methods for the Examination of Water and Wastewater, 20th Ed. Washington, D.C.

Barbieri, M., Morotti, M., 2003. Hydrogeochemistry and strontium isotopes of spring and mineral waters from Monte Vulture volcano, Italy. Appl. Geochem. 18, 117–125.

Basu, A.R., Jacobsen, S.B., Poreda, R.J., Dowling, C.B., Aggarwal, P.K., 2001. Large groundwater strontium flux to the oceans from the bengal basin and the marine strontium isotope record. Science 293 (5534), 1470–1473. https://doi.org/10.1126/science.1060524.

Bauer-Gottwein, P., Gondwe, B.R.N., Charvet, G., et al., 2011. Review: The Yucatán Peninsula karst aquifer, Mexico. Hydrogeol. J. 19, 507–524. https://doi.org/10.1007/s10040-010-0699-5.

Beck, A.J., Charette, M.A., Cochran, J.K., Gonneea, M.E., Peucker-Ehrenbrink, B., 2013. Dissolved strontium in the subterranean estuary - implications for the marine strontium isotope Budget. Goechimica et Cosmochimica Acta 117, 33–52. https://doi.org/10.1016/j.gca.2013.03.021.

Blum, J.D., Erel, Y., 2005. Radiogenic isotopes in weathering and hydrology. In: Drever, J.I. (Ed.), Surface and Ground Water, Weathering, and Soils. Treatise on Geochemistry. Elsevier, pp. 365–392.

Capo, R., Stewart, B., Chadwick, O., 1998. Strontium isotopes as tracers of ecosystem processes: theory and methods. Geoderma 82, 197–225.

Chakrabarti, R., Mondal, S., Acharya, S.S., Lekha, J.S., Sengupta, D., 2018. Submarine groundwater discharge derived strontium from the Bengal Basin traced in Bay of Bengal water samples. Scientific Reports 8(4383). https://doi.org/10.1038/s41598-018-22299-5.

Clow, D.W., Mast, M.A., Bullen, T.D., Turk, J.T., 1997. Strontium 87/strontium 86 as a tracer of mineral weathering reactions and calcium sources in an alpine/subalpine watershed, Loch Vale, Colorado. Water Resour. Res. 33, 1335–1351.

Gilli, A., Hodell, D.A., Kamenov, G.D., Brenner, M., 2009. Geological and archaeological implications of strontium isotope analysis of exposed bedrock in the Chicxulub crater basin, northwestern Yucatán, Mexico. Geol. 37 (8), 723–726. https://doi.org/10.1130/G30098A.1.

Gondwe, B., Lerer, S., Stisen, S., Marín, L., Rebolledo-Vieyra, M., Merediz-Alonso, G., Bauer-Gottwein, P., 2010. Hydrogeology of the southeastern Yucatán Peninsula: new insights from water level measurements, geochemistry, geophysics and remote sensing. J. Hydrol. 389 (1), 1–17. https://doi.org/10.1016/j.jhydrol.2010.04.044.

Graustein, W.C., 1989. $^{87}Sr/^{86}Sr$ Ratios Measure the Sources and Flow of Strontium in Terrestrial Ecosystems. In: Rundel, P.W., Ehleringer, J.R., Nagy, K.A. (Eds.), Stable Isotopes in Ecological Research. Springer, Berlin Heidelberg New York, pp. 491–512.

Hernández-Terrones, L.M., Null, K.A., Ortega-Camacho, D., Paytan, A., 2015. Water quality assessment in the Mexican Caribbean: impacts on the coastal ecosystem. Continent. Shelf Res. 102 (1), 62–72.

Hernández-Terrones, L., Rebolledo-Vieyra, M., Merino-Ibarra, M., Soto, M., Le-Cossec, A., Monroy-Rios, E., 2011. Groundwater pollution in a karstic region (NE Yucatán): baseline nutrient content and flux to coastal ecosystems. Water Air Soil Pollut. 218, 517–528. https://doi.org/10.1007/s11270-010-0664-x.

Herrera-Silveira, J.A., Morales-Ojeda, S.M., 2009. Evaluation of the health status of a coastal ecosystem in southeast Mexico: assessment of water quality, phytoplankton and submerged aquatic vegetation. Mar. Pollut. Bull. 59, 72–86. https://doi.org/10.1016/j.marpolbul.2008.11.017.

Hodell, D.A., Quinn, R.L., Brenner, M., Kamenov, G., 2004. Spatial variation of strontium isotopes ($^{87}Sr/^{86}Sr$) in the Maya region: a tool for tracking ancient human migration. J. Archaeol. Sci. 31, 585–601.

Holmden, C., Papanastassiou, D.A., Blanchon, P., Evans, S., 2012. Δ44/40Ca variability in shallow water carbonates and the impact of submarine groundwater discharge on Ca-cycling in marine environments. Geochem. Cosmochim. Acta 83, 179–194.

Instituto Nacional de Estadistica y Geografia, 2010. www.inegi.org.mx.

Jones, B.F., Vengosh, A., Rosenthal, E., Yechieli, Y., 1999. In: Bear, J., et al. (Eds.), Geochemical Investigations in Seawater Intrusion in Coastal Aquifers-Concepts, Methods and Practices, pp. 43–63 (Kluwer Acad., Norwell, Mass).

Katz, B.G., Bullen, T.D., 1996. The combined use of $^{87}Sr/^{86}Sr$ and carbon and water isotopes to study the hydrochemical interaction between groundwater and lakewater in a mantled karst. Geochem. Cosmochim. Acta 60, 5075–5087.

Lopez-Ramos, E., 1975. Geological summary of the Yucatan peninsula. In: Nairn, A.E.M., Stehli, F.G. (Eds.), The Ocean Basins and Margins, the Gulf of Mexico and the Caribbean, vol. 3. Plenum Press, NY, USA (Chapter 7).

McArthur, J.M., Howarth, R.K., Bailey, T.R., 2001. Strontium isotope stratigraphy: LOWESS Version 3; best fit to the marine Sr-isotope curve for 0-509 Ma and accompanying look-up table for deriving numerical age. J. Geol. 109, 155–170.

McArthur, J.M., Donovan, D.T., Thirlwall, M.F., Fouke, B.W., Mattey, S., 2000. Strontium isotope profile of the early Toarcian (Jurassic) oceanic anoxic event, the duration of ammonite biozones, and belemnite palaeotemperatures. Earth Planet Sci. Lett. 179, 269–285.

Moore, W.S., 1999. The subterranean estuary: a reaction zone of ground water and seawater. Mar. Chem. 65, 111–125.

Mutchler, T., Dunton, K.H., Townsend-Small, A., Fredriksen, S., Rasser, M.K., 2007. Isotopic and elemental indicators of nutrient sources and status of coastal habitats in the Caribbean Sea, Yucatán Peninsula, Mexico. Estuar. Coast Shelf Sci. 74, 449–457.

Négrel, P., Petelet-Giraud, E., 2005. Strontium isotopes as tracers of groundwater-induced floods: the Somme case study. J. Hydrol. 205, 99–119.

Null, K.A., Knee, K.L., Crook, E., de Sieyes, N., Rebolledo-Vieyra, M., Hernández-Terrones, L., Paytan, A., 2014. Composition and fluxes of submarine groundwater along the Caribbean coast of the Yucatan Peninsula. Continent. Shelf Res. 77 (2014), 38–50. https://doi.org/10.1016/j.csr.2014.01.011.

Paytan, A., Kastner, M., Martin, E.E., Macdougall, J.D., Herbert, T., 1993. Marine barite as a monitor of seawater strontium isotope composition. Nature 366, 445–449.

Perry, E., Paytan, A., Pedersen, B., Velazquez-Oliman, G., 2009. Groundwater geochemistry of the Yucatan peninsula, Mexico: constraints on stratigraphy and hydrogeology. J. Hydrol. 367, 27–40.

Perry, E., Velazquez-Oliman, G., Marin, L., 2002. The hydrogeochemistry of the karst aquifer system of the northern Yucatan Peninsula, Mexico,. Int. Geol. Rev. 44, 191–221.

Perry, E.C., Swift, J., Gamboa, J., Reeve, A., Sanbonr, R., Marín, L.E., Villasuso, M., 1989. Environmental aspects of surface cementation, north coast, Yucatan, Mexico. Geology 17, 818–821.

Pilson, M.E.Q., 2013. An Introduction to the Chemistry of the Sea, second ed. Cambridge University Press, New York. 524 pp.

Pu, J., Yuan, D., Zhang, C., Zhao, H., 2012. Tracing the sources of strontium in karst groundwater in Chongqing, China: a combined hydrogeochemical approach and strontium isotope. Environ Earth Sci 67, 2371–2381.

Rahaman, W., Singh, S.K., 2012. Sr and $^{87}Sr/^{86}Sr$ in estuaries of western India: impact of submarine groundwater discharge. Geochem. Cosmochim. Acta 85, 275–288.

Secretaría de Turismo de Quintana Roo, 2015. www.sedetur.qroo.gob.mx.

SGM, 2007. Carta geológica de México [Geological map of Mexico]. Escala 1:2,000,000, 6th edn., Servicio Geológico Mexicano (SGM). Pachua, Mexico.

Shand, P., Darbyshire, D.P.F., Love, A.J., Edmunds, W.M., 2009. Sr isotopes in natural waters: applications to source characterization and water-rock interaction in contrasting landscapes. Appl. Geochem. 24, 574–586.

Singurindy, O., Berkowitz, B., Lowell, R.P., 2004. Carbonate dissolution and precipitation in coastal environments: laboratory analysis and theoretical consideration. Water Resour. Res. 40 https://doi.org/10.1029/2003WR002651. W04401.

Tobón-Velázquez, N.I., Rebolledo-Vieyra, M., Paytan, A., Broach, K.H., Hernández-Terrones, L.M., 2018. Hydrochemistry and carbonate sediment characterization of bacalar lagoon, Mexican Caribbean. Marine and Freshwater Research, doi. https://doi.org/10.1071/MF18035.

Veizer, J., 1989. Strontium isotopes in seawater through time. Annu. Rev. Earth Planet Sci. 17, 141–167.

Vengosh, A., Gill, J., Davisson, M.L., Huddon, G.B., 2002. A multi isotope (B, Sr, O, H, C) and age dating (^{3}H-^{3}He, ^{14}C) study of groundwater from Salinas Valley, California: hydrochemistry, dynamics, and contamination processes. Water Resour. Res. 38 (9), 1–17.